UVM 2021 Lake Carmi Monitoring Report to Vermont DEC

Authors: Andrew Schroth, Mindy Morales-Wiliams, Ashton Kirol, Kris Stepenuck

Key Findings:

● When functional, the aeration system has substantially decreased Lake Carmi's water column stability, making it more prone to mixing, and likely suppressing some internal phosphorus loading from sediments.

● Multiple aeration system malfunctions in 2021 (and in previous years) makes it impossible for comprehensive assessment of the system's capacity to achieve its water quality goals with respect to water column phosphorus concentration or cyanobacteria bloom occurrence, duration or severity.

● In 2021, sustained anoxic conditions at the sediment-water interface associated with aeration system failures triggered periods of relatively high levels of internal phosphorus (P) loading (compared to 2020). With subsequent wind/aerator induced mixing of the sediment-derived P, the entire water column had P concentrations over twice the TMDL target concentration for much of the summer and fall.

● There is increased evidence that even the partially functional aeration system has changed cyanobacteria bloom composition, timing and biomass. There was no significant difference in overall phytoplankton biomass post aeration intervention in 2019 and 2020, but overall biomass did increase significantly compared to previous monitored years in 2021. Further, cyanobacteria and diatom biomass increased in 2020 and 2021 relative to previous years. In 2021, diatoms did not change relative to the previous year, but cyanobacteria biomass did, driving the overall biomass increase. These increases were dominated by nitrogen fixing taxa (*Aphanizomenon flos-aquae*, *Dolichospermum spp.*), suggesting the aeration system has exacerbated existing nitrogen limitation.

Introduction: 2021 was the third year of the aeration intervention in Lake Carmi aimed at suppressing anoxic conditions at the bottom of the lake to limit internal loading of phosphorus (P) from the lake's sediments. Here, we present preliminary results from the second monitoring year of our research project. Where relevant, we compare data from 2021 to pre-aeration (mostly 2018 when UVM had fixed oxygen and temperature sensors deployed in the lake) and also to some observations from other aeration years (2019, 2020). As in 2019 and 2020, intermittent multi-day malfunctions of the aeration system in 2021 compromised our ability to fully assess the capacity of the system to alter Lake Carmi's water quality and ecology. However, we have detected substantial changes to the lake's chemical and ecological systems, facilitated by inconsistent aeration, which are discussed here. In general, the timing, duration and nature of system fluctuations in performance and how they relate to the weather and conditions in the lake,

drove the behavior of phosphorus and impacted the occurrence of cyanobacteria blooms. Our report first discusses weather and climate observations of 2021 for context. We then discuss how the aeration impacted the thermal and oxygen profiles of the lake and the impact of wind on fully mixing the system. This is followed by a discussion of nutrient and metal time series data collected by both UVM and VT DEC, focusing on the extent to which geochemical signatures of internal loading were detected in 2022, and how that compares to historical time series data collected by VT DEC and UVM. Our final section discusses processed biological time series data from both sensors (2020, 2021) and integrated water samples (2018-2021). In all cases, analysis should be considered preliminary, and substantial additional analysis will occur over the remaining 1.5 years of the project. This report is designed to provide VT DEC practitioners and other partners our synopsis of what we have observed thus far and tentative inferences that can be drawn.

2021 Aeration system functionality summary: The aeration system consists of two broadly distributed arrays, one that is fed by a compressor at the state park (herein refered to as the 'southern array'), the other fed by an air compressor on the Evans property (herein reffered to as the 'northern array). The entire system was turned on May 19th after initial development of stratification was observed and thermal and DO thresholds were reached (15 degr. C. 5.0 mg/L DO); the earliest initiation of aeration yet for this site. Both arrays were working, but the southern (State Park) system was not running to specifications due to an undetected leak underground. Two diffusers were down completely. Maintenance was done on the diffusers from 5/31 to 6/2. Additional maintenance was perfomed on the southern system on June 7-9. All diffusers were working, but still at a lesser rate than the northern (Evans) array. On 6/21 the main line failed on the southern system and was shut down completely. The northern array also failed on 6/28, and the entire aeration system was down until July 1st when repairs were made. The northern array failed again between August 6th and 12th, and a final time on October 3rd when it was shut down for the season. The southern array was shut down for the season on October 5th.

2021 Meteorology: From a climate and weather perspective, 2021 was particularly notable because of the sustained drought conditions in northern Vermont. This is illustrated in Figure 1 where cumulative precipitation was below normal from March through the remainder of the year. Indeed, these conditions were a continuation of drought conditions from 2020, and NOAA indicates that this was part of a 73 week period of drought conditions in Vermont that spanned June 23, 2020 through October 26th 2021, the longest drought period on record for Vermont in the 21st century (https://www.drought.gov/states/vermont). These are conditions conducive to substantial internal loading of legacy phosphorus in lake sediments into the lake driving lake phosphorus concentrations given low inputs of water from contributing watersheds. Notable periods of particular warmth in 2021 included late March and early April, much of June, late August and early September, as well as much of October. There were also larger summer high flow events in the watershed in 2020 than in 2021 as indicated by the Pike River hydrograph (Figure 2).

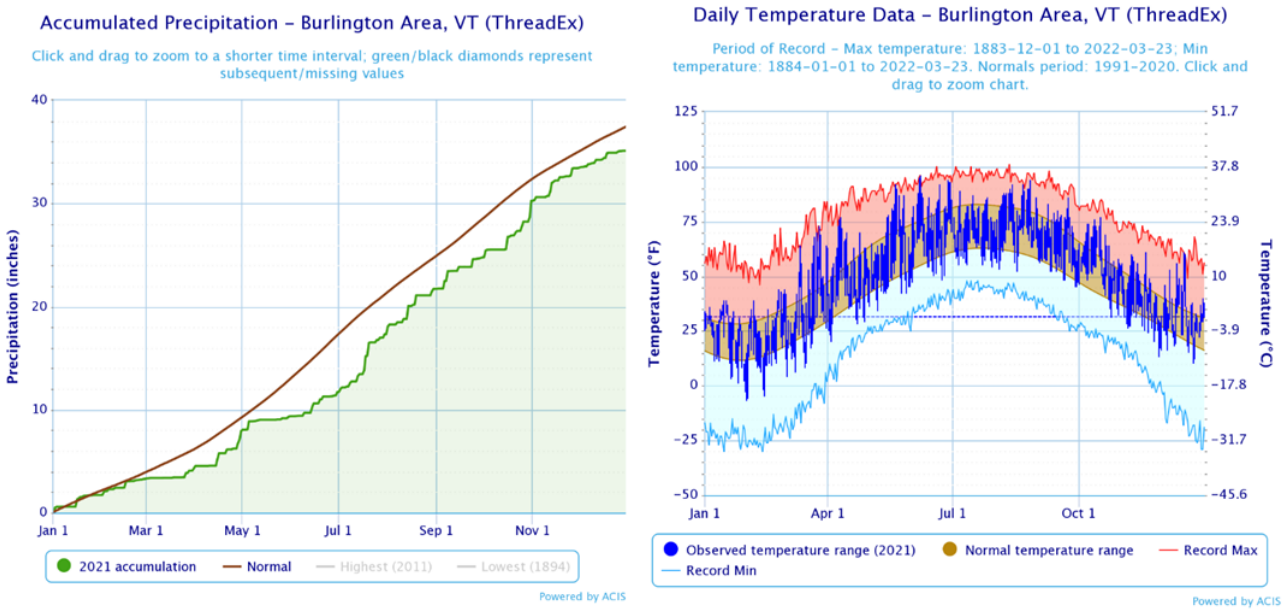

Figure 1: 2021 cumulative precipitation and daily temperature measurements from Burlington, VT (source NOAA). Note, Burlington accumulated precipitation is an underestimate of drought conditions observed in more northern portions of Vermont where many tributaries dried up completely for extended periods of time. For example, the USGS gage at Franklin County's Jewett Brook (St. Albans) recorded no measurable flow from June 7th until October 26th of 2021 (https://waterdata.usgs.gov/monitoring-location/04292810/#parameterCode=00060&period=P365D).

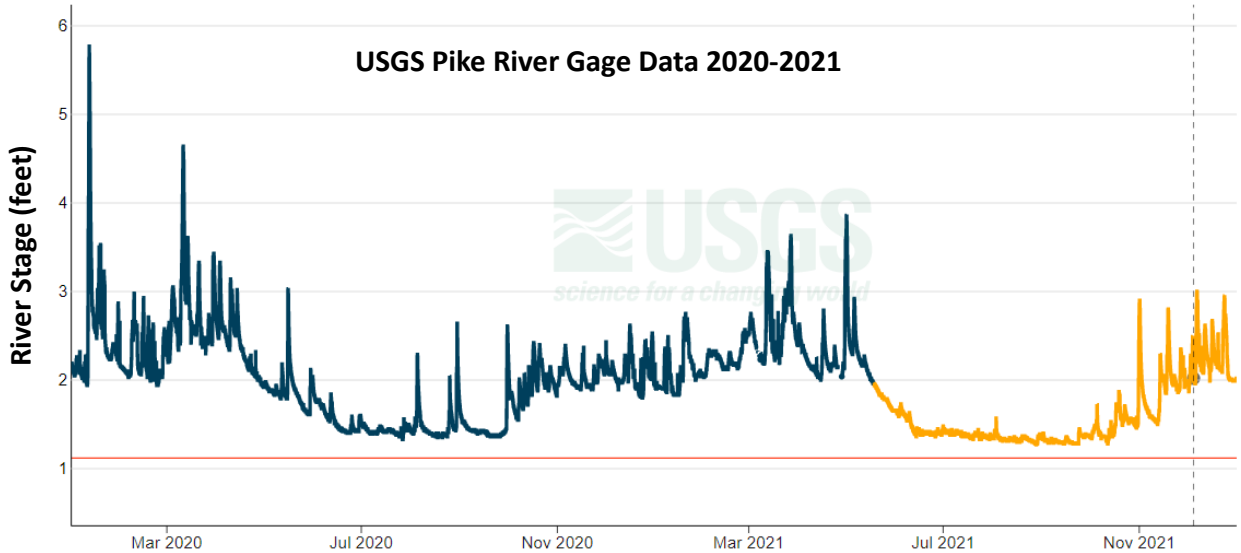

Figure 2: USGS Gauge Pike River stage data from the Pike River showing very few summer high flow events in 2021, even relative to the preceding dry summer of 2020. This indicates low

levels of watershed-derived nutrient loading during summer months. Blue lines are certified USGS data, whereas yellow lines remain provisional date yet to be certified.

Water temperature and thermal stratification and stability: Water temperature data from 2021 indicates that the relatively warm period of late March and early April allowed Carmi's waters to rise above the thermal threshold for walleye fry by early May, with thermal stratification also setting up during this period (Figure 3). As such the aeration system was turned on relatively early on May 19th. Bottom water temperatures then began to rise as aeration facilitated partial mixing with warmer waters near the surface (Figure 3), and water column stability broke down (Figure 4) over time with a wind-enhanced mixing event then facilitating turnover of the water column near the end of the month. Unfortunately, this event corresponded with a series of limited to non-functionality of the system for what constituted most of June (see above section on aeration). The system's non-functionality then led to sustained thermal stratification developing for most of June, which was eventually broken down by the strongest wind event of the monitoring season at the end of the month (Figures 3,4). However, the northern array then also shut down, and thermal stratification was re-established until the aerators were fixed combined with another wind event facilitated full water column turnover. With both systems functioning for July, we saw very similar stratification and stability dynamics as we saw in 2020 with the fully functioning system; the water column was extremely dynamic with a relatively low stability, oscillating between low level stability and stratification (e.g. ~1 degree difference between bottom and surface water temperatures) and isothermal and fully mixed by relatively low level wind events (Figures 3,4). This is in stark contrast to the 2018 pre-aeration water column stability where we see sustained thermal stratification and high-water column stability throughout the summer until fall turnover (Figure 4). The bottom water temperature over this period was quite consistent at just around 22 ºC, roughly 5 ºC warmer than the pre-aeration summer bottom water temperature of around 17 ºC. There was then another early August shutdown of the northern array, and thermal stratification rapidly became more pronounced (2-3 ºC differences between bottom and surface) for the rest of the month. During this period, surface water temperatures reached their maximum readings for the summer season around 25 ºC, slightly below the previous summer's high temperature. Water temperatures stayed in this range for much of the second half of August, until the lake turned over due to a wind event at the end of the month. For the first portion of September, due to a combination of frequent high wind events, cooling air temperatures, and a fully functioning aerator, the water column was mostly isothermal and cooling. There was a weeklong period of low wind and warm temperatures in the middle of September where temperature cooling plateaued and minor stratification (~1 ºC redeveloped, even with a fully functioning aeration system. However, after the aerator was shut down on October 3rd, there was a final sustained warm period with relatively calm winds early in the month that allowed for surface waters to warm and stratification to redevelop for the first half of the month, also interrupting the overall fall trend of cooling waters. The latter half of October then became cooler, relatively windy, and the water column remained mixed and unstable for the remaining of the monitoring period, as the platform was pulled in early November. Figure 3 below is a nice illustration of how the aerator changed

the water column stability relative to the pre-aeration hydrodynamic system and illustrates not only how dynamic and unstable the water column can become when the system is functioning, but also how quickly it can recover in response to partial or full shutdowns of the array. Interannual differences in the timing and duration of system shutdowns are also clearly evident when comparing water column stability time series between 2020 and 2021.

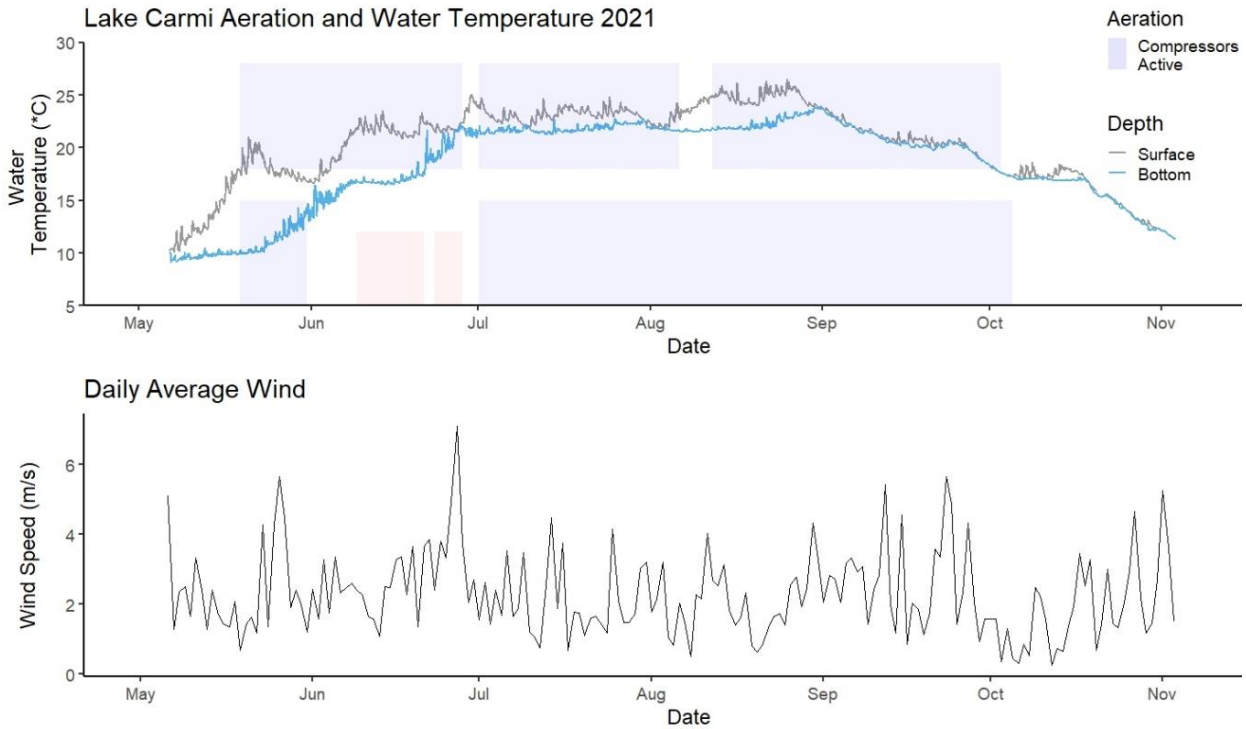

Figure 3: Bottom and surface high frequency (collects data at 15-minute intervals) temperature time series from the 2021 monitoring period and concurrent wind measurements from the platform. In the upper panel, blue regions indicate a mostly functional, pink areas indicate partial but suboptimal aerator functionality, whereas white areas indicate the system is shut down.

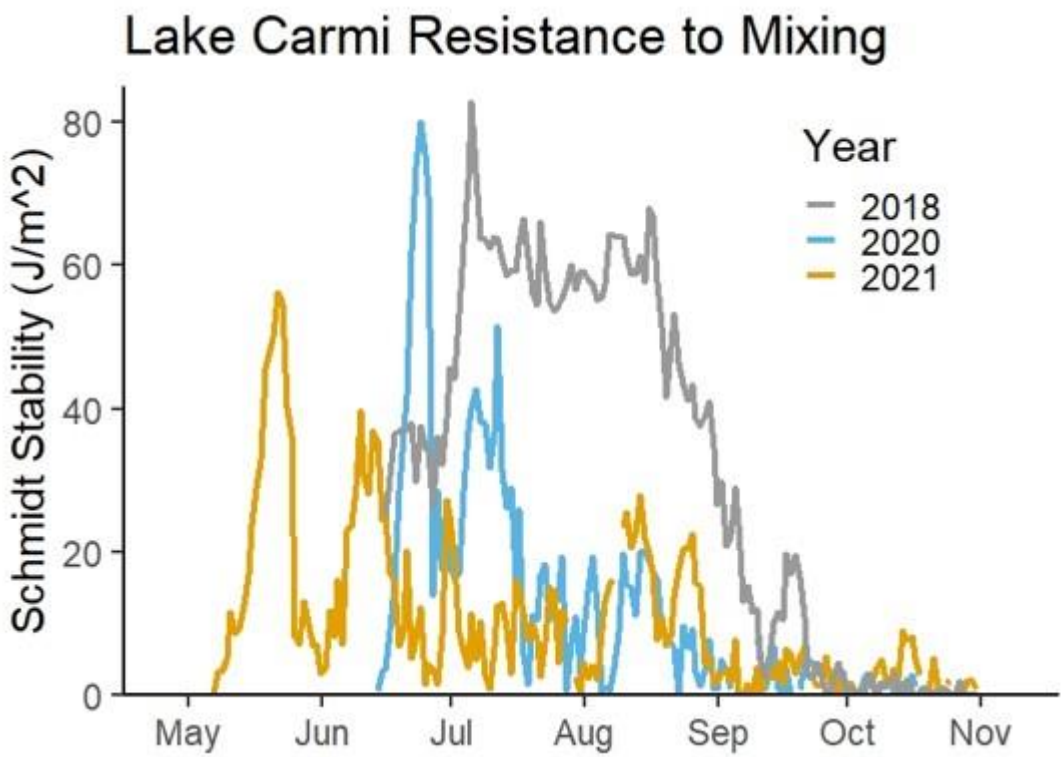

Figure 4: Schmidt water column stability estimates derived from thermistor chains at the same location in 2018 (pre-aeration), 2020 and 2021. Higher stability numbers indicate higher energy. (wind) is needed to mix the water column, whereas lower numbers require less wind to facilitate mixing (zero is isothermal and well-mixed). Note that fluctuations in stability in 2020 and 2021 are driven by a combination of the ambient weather (temperature and wind) and the performance of the aerator. Periods with high values are associated with aerator malfunctions during the spring and summer, which occurred at different times of the year in each monitoring season.

2021 Dissolved oxygen dynamics: By turning on the system in early May 19thwhen bottom water oxygen concentrations were well over the threshold of 2.5 mg/L, the system was able to mix and oxygenate the water column (with facilitation by a relatively strong wind event) and keep the bottom water from reaching the threshold during early operation (Figure 5). This demonstrates that there is the potential to keep the lakebed from reaching and going below the DO threshold if the aerators are turned on at an early stage of thermal stratification development in spring (note that the system was not turned on in time to prevent the low DO threshold from being breached in the previous two years). We recommend that those responsible for management and operations should be poised to utilize the high frequency real time data to ascertain when the system has reached temperature thresholds for walleye fry and operators should be prepared to rapidly respond by turning on the aeration system.

Unfortunately, maintenance of high oxygen concentrations in bottom waters was short lived, as with southern array failure, the bottom water dissolved oxygen rapidly plummeted and ultimately went anoxic for much of the second half of the month (Figure 5). During July, bottom water oxygen concentrations were fluctuating between anoxic and completely unstratified with very

rapid changes between those two states in response to changes in wind and an unstable water column (Figures 3,4,5). This is very similar to what we see in Missisquoi Bay naturally during the summer, where subtle changes in wind speed and orientation exert a strong control on bottom water oxygen concentrations on very short (hourly) timescales due to a combination of an unstable water column and a high sediment oxygen demand associated with relatively warm bottom water and ample nutrients. There was another period of sustained anoxia for much of August in response to the northern array shutting down and the re-establishment of sustained thermal stratification and increased water column stability suppressing low level wind induced mixing. Bottom water anoxia was prolonged by a period of low wind following the fixes to aeration, which sustained stratification and limited mixing. With sustained mixing of September waters with fully functioning aerator and cooling waters, generally oxygen concentration throughout the water column decreased as is typical as lake water cooled. While the bottom water never dipped below the DO target for a sustained period of time, brief rapid plunges in bottom water DO were still evident when winds subsided in September (Figures 3, 5). Importantly, after the aerator was shut down in early October a late season heat wave and low wind event allowed stratification to redevelop, and the sediment again went anoxic briefly. To avoid such a situation in the future, we would suggest that operators and VT DEC consider long-term forecasts and current water temperatures when deciding to turn the system off. If financially feasible, given Carmi's history of fall cyanobacteria blooms, it is worth considering keeping the system on well into October, particularly if the water is warm and blooms have been established and prevalent in late summer.

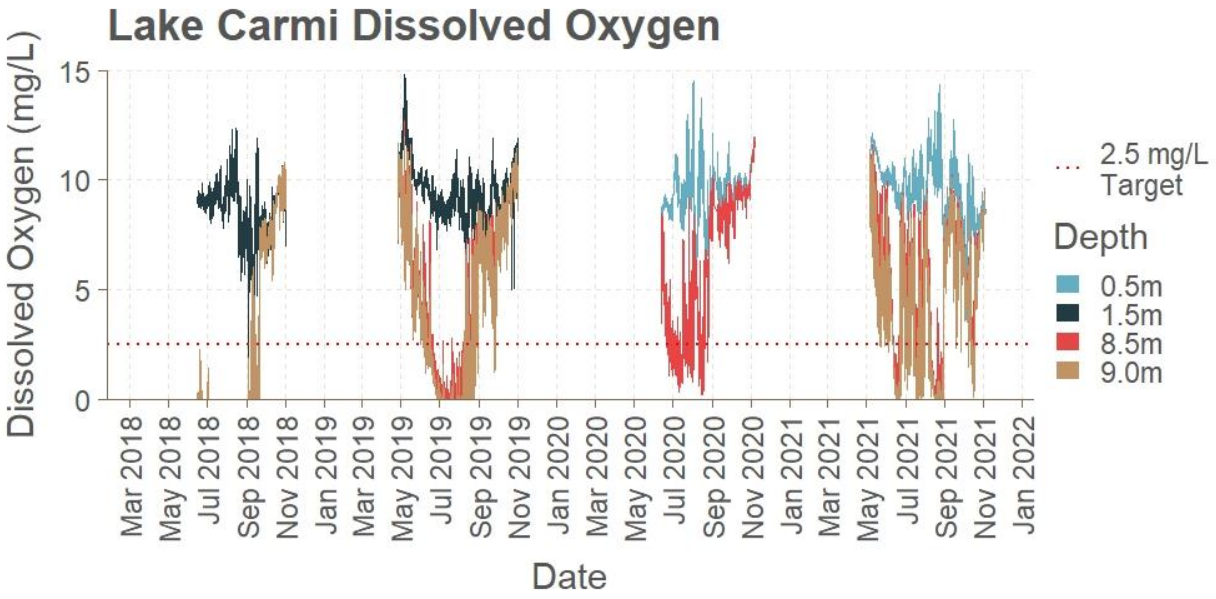

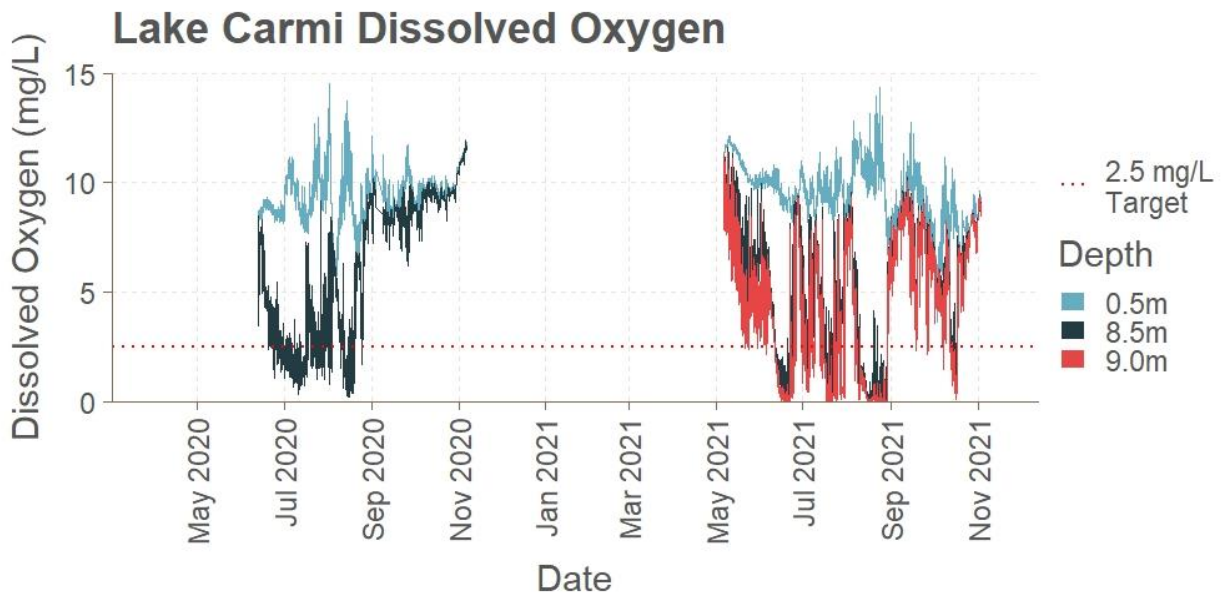

Figure 5: High frequency dissolved oxygen time series at different depths from fixed HOBO dissolved oxygen sensors since deployment in 2018 (upper plot) and just data from 2020 and 2021 in lower plot to better illustrate observed differences between the two. Target of 2.5 mg/L shown in red dot line at a depth of 8.5 meters (black line).

Water column phosphorus and manganese: Similar to the 2019 and 2020 seasons, there is substantial evidence of intermittent internal loading based on the bottom water time series, which is less evident in the DEC dataset where the deepest sample is still almost a meter off the bottom of the water. Spikes in the concentration of bottom water P occur during sustained periods of bottom water being below the DO threshold (Figures 5,6). There is substantial fluctuation in the bottom water P data, which could be due to fluctuating levels of internal P loading, subtle changes in the depth of the intake tubing due to wave action, changing water levels, and even disturbance/vertical mixing of the flocculant layer around the sediment water interface, thus individual daily spikes in P concentration should not be over emphasized. In a second water P concentration plot, Figure 7we eliminated the particularly high concentration outliers to allow for focus on the overall trend in the bottom water samples relative to the DEC data. The systematic offset of increasing P concentrations clearly illustrates the lag in response of the upper water column (DEC red and yellow datapoints) to P loading from the sediment (UVM blue datapoints), but the fact that the general seasonal pattern is the same indicates that internal loading is the dominant culprit for elevated P concentrations in the water column (Figures 6,7). In the VT DEC dataset, we also see similarities to the previous two seasons under aeration, where the earliest signals of internal loading are detected after aeration-induced mixing of the P enriched bottom water raises the concentration of P in the entire water column well above the TMDL target concentration (Figure 6). We do note additional evidence of internal loading in the DEC dataset more akin to observations preceding aeration where their deepest samples were enriched in P (relative to the samples collected in shallower portions of the water column) during the second anoxic bottom water period in late August (DEC did not detect P stratification in their

data in 2020-Figure 6). Furthermore, similar to 2020, the DEC manganese (Mn) dataset show high levels of Mn during periods of enriched bottom water phosphorus, and the temporal structure of the Mn time series is quite similar to that of phosphorus (Figure 7). Mn is a strong proxy for redox induced release of P from sediments. The higher Mn concentrations and stratification in the DEC dataset relative to those observed in 2020 further suggests that there was more internal loading in the 2021 monitoring season. Indeed, in 2021 there were few storms detected in the Pike River hydrograph (Figure 2), and the concentrations of P in the lake during spring runoff, where the watershed is the dominant source of P, are in fact some of the lowest of the monitoring season-a seasonal trend to that is clear throughout the monitoring time series (Figure 6). The limited precipitation within the small watershed during this drought summer, coupled with the previously mentioned signals of internal loading during anoxic intervals triggered by aeration failure suggest the internal loading was likely the primary driver of increasing and high P concentrations through much of the summer and fall bloom season.

To be clear, this does not suggest that prioritizing substantial reductions in phosphorus loading from the watershed is not the long-term solution to meeting the TMDL and suppressing cyanobacteria blooms in Lake Carmi. In fact, reducing phosphorus loading from watershed sources is **the essential long-term** solution to making the investment in the aeration system worthwhile and sustaining clean water in Carmi. However, the seasonal patterns that we see in post aeration years of building summer P over time has primarily been due to internal loading triggered by fluctuations in aerator performance. The critical question that remains unanswered is that *if* the aerator can remain fully functional during the summer, can Carmi maintain phosphorus concnetrations remain similar to those of late spring rather than allowing them to roughly double later in the summer?

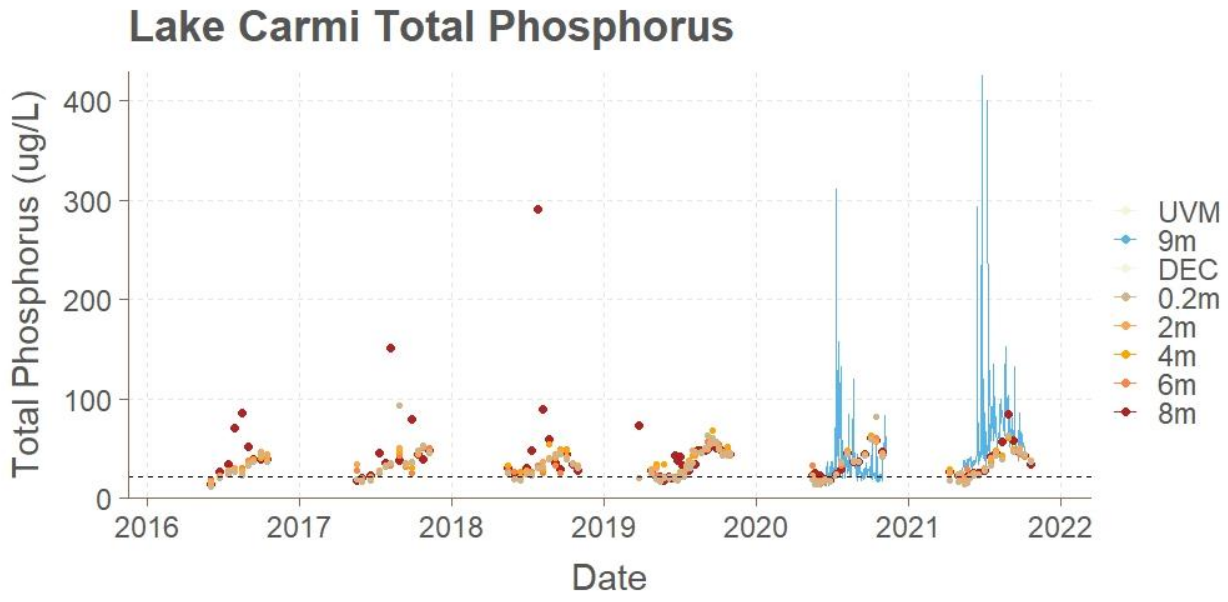

Figure 6: Vermont DEC total P time series (mostly biweekly) from 2016 to 2022, with UVM high frequency (daily) bottom water time series in blue. TMDL target concentration of 22 ug/L TP shown in red.

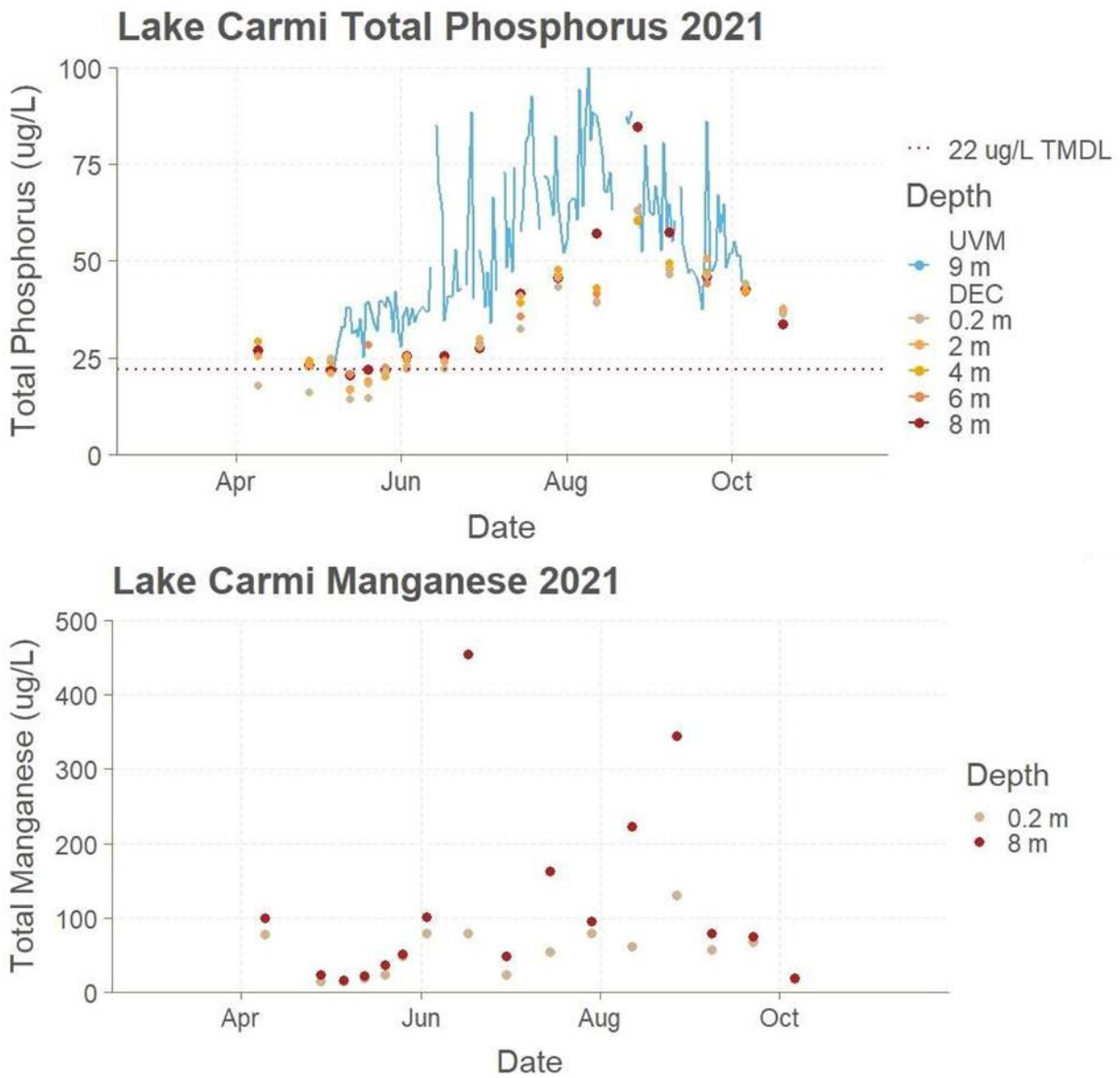

Figure 7: Vermont DEC Total P (upper plot red and yellow points) and total Mn (bottom plot) biweekly time series. UVM TP data with high outlier concentrations removed to decrease the scale of the Y axis to illustrate the dominant trends in the majority of the data**.**

Sediment phosphorus: In general, sediment concentrations of phosphorus were similar to those measured in sediments collected during the 2020 sediment sampling campaign (Figure 8). Sediment collected during 2021 also bear similar overall patterns of decreasing concentrations of sediment total and reactive P with increasing depth within the sediment profile (Figure 8). There is evidence of internal loading of reactive sediment P pools (decreasing concentrations of

sediment reactive P between sediment sampling time points) that in general correspond to periods of anoxic sediment-water interface conditions captured in early June, August, and October. These periods of loss are most evident in the upper 2 centimeters of sediment, which would be the portion of the sediment profile that would be contributing most to water column P fluxes, and also most sensitive to fluctuations in overlying water column fluctuations in redox conditions. This further supports the water column data that indicated that there was increased internal P loading during the monitoring period of 2021 relative to that of 2020, likely due to the more extreme and frequent low oxygen conditions that were observed during that year discussed earlier in this report (Figure 5).

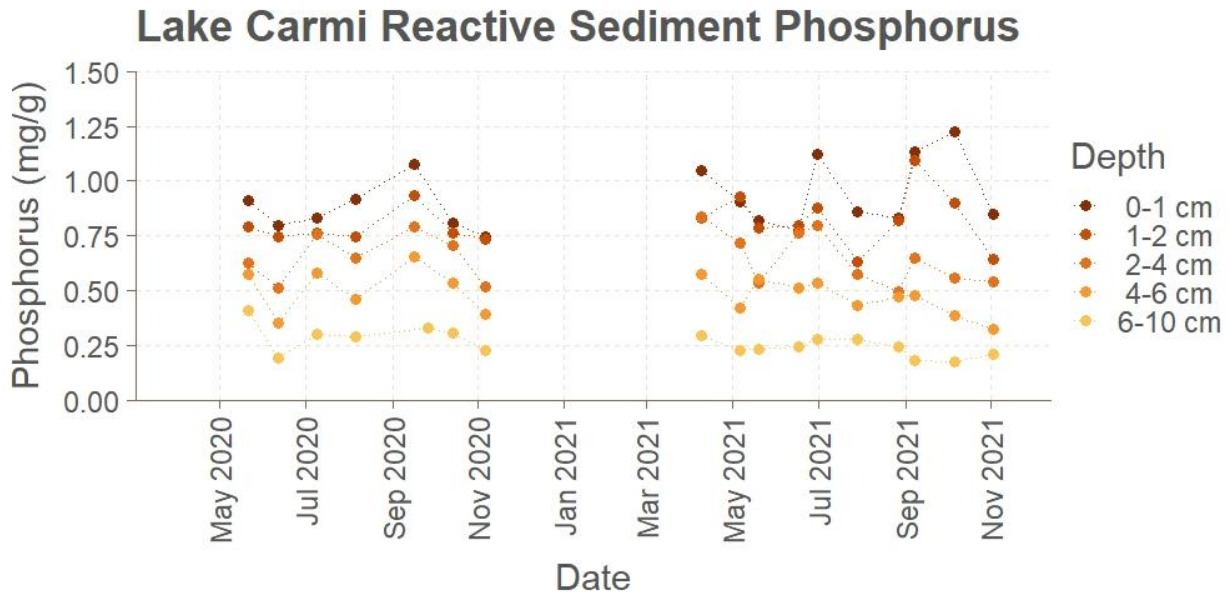

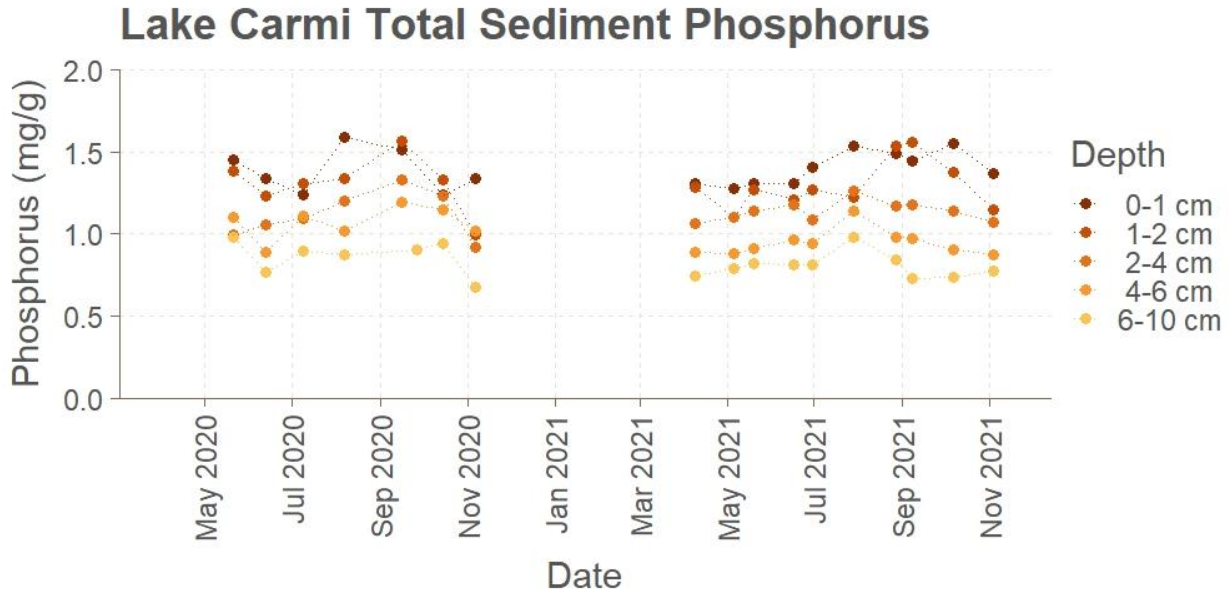

Figure 8: Biweekly sediment phosphorus time series from 2021 and 2022 from 5 depth intervals. The upper plot labeled Reactive P' is derived from an ascorbate extraction that targets the pool of phosphorus that would be released during low oxygen conditions in the sediment. The lower plot are concentrations derived from an aqua regia digestion that dissolves most forms of phosphorus including less reactive crystalline minerals and recalcitrant organic forms that are less likely to contribute to water column P fluxes.

Biological pigments and phytoplankton data: In 2021 phycocyanin levels slowly increased from late June through July and peaked in August following a mixing event that was preceded by sustained anoxia at the sediment water interface (Figures 5,9). This phycocyanin peak also coincided with the warmest water temperatures of the year above 25 ºC (Figures 3,9). Sustained relatively high levels of phycocyanin persisted through the rest of the monitoring period into October. Our sensor was compromised for the last half of that month due to presumed biological fouling, but field research visual estimates was that the bloom was not visually apparent by the last field sampling data, suggesting that over this period of more intense bloom conditions subsided.

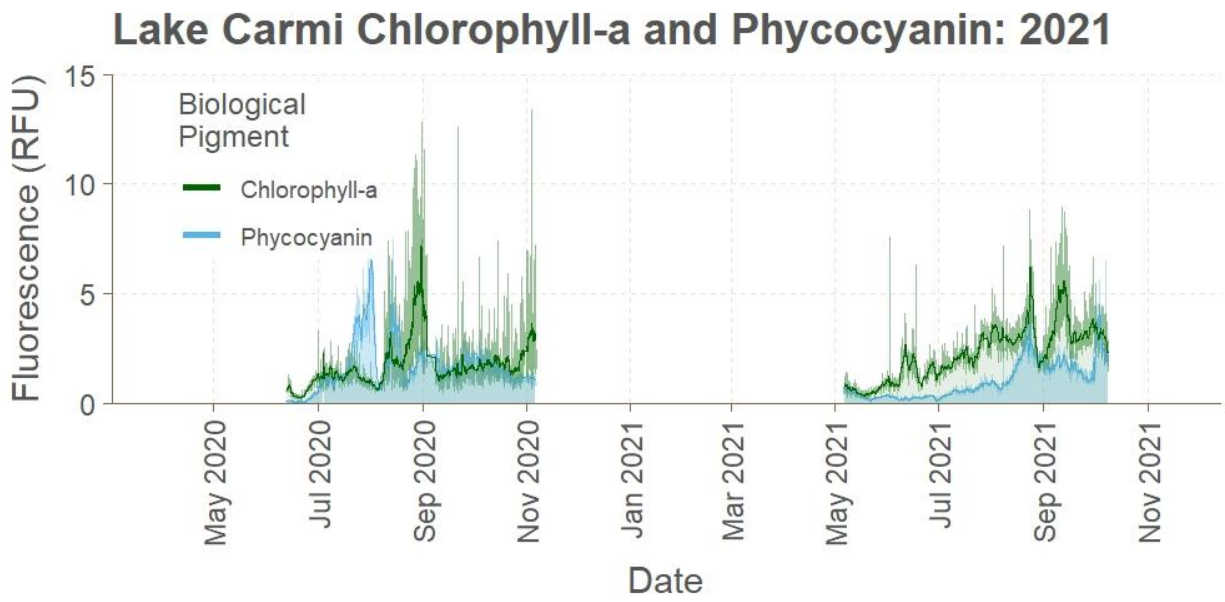

Figure 9. Time series of high-frequency biological pigment measurements in 2020 and 2021. Showing peaks in phycocyanin in July and August 2020, and later in August and September in 2021.

Phytoplankton biomass and community composition: We found no significant difference in overall phytoplankton biomass in 2020 relative to 2019 or pre-aeration 2018, but there was an overall biomass increase in 2021 (Figure 10). However, in 2020, both cyanobacteria and diatom (Bacillariophyta) biomass increased relative to previous years (Figure 11), and in 2021 cyanobacteria increased again driving the overall phytoplankton biomass increase. In addition, community composition shifted in 2020 (Figure 11) and 2021.

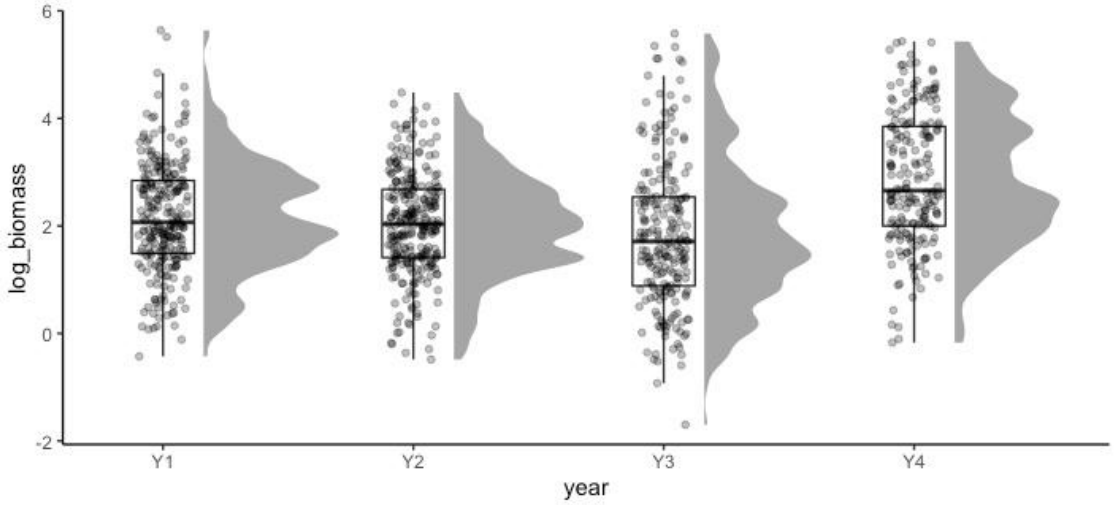

Figure 10. Log transformed overall phytoplankton biomass for all sampling events in Lake Carmi between 2018 (Y1) – 2021 (Y4). These data indicate high variability in biomass between sampling events in 2020 and 2021 relative to other years, and a significant overall increase in biomass in 2021 following no change in previous years 1-3.

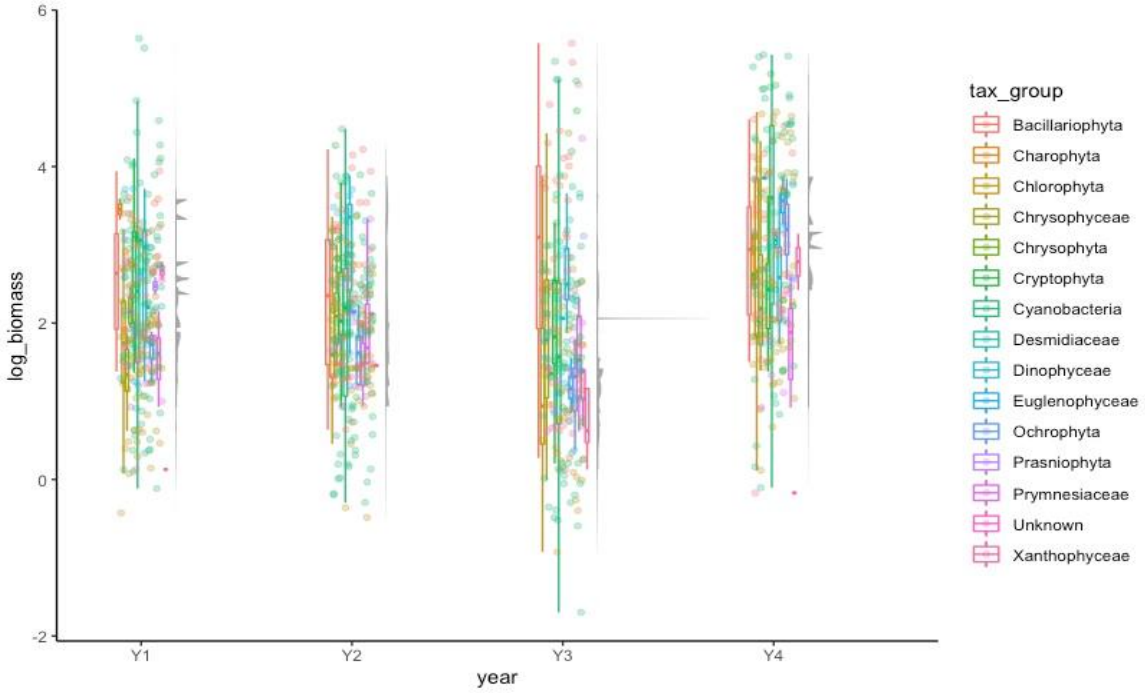

Figure 11. Log transformed biomass visualized by taxonomic group, showing a significant increase in diatom (Bacillariophyta) and cyanobacteria biomass in year 3 (2020) relative to previous years, and an increase in cyanobacteria biomass in 2021.

Carmi has been consistently dominated by nitrogen fixing taxa throughout the monitoring period, though dominant taxa have fluctuated each year. Specifically, in **2018** (pre-aeration), early season blooms were dominated by multiple *Dolichospermum* spp., then shifted to *Cuspidothrix elenkinii* later in the season, followed by growth of non-N-fixing coccoid taxa (*Woronichinia naegeliana* and *Aphanocapsa* sp.) at non-bloom concentrations in the fall (Figure 12a). Pre-aeration **2019** communities were similar to early 2018, with the addition of a large N-fixing filamentous taxa known to form toxic surface scums, *Limnoraphis birgei*. Immediately following aeration, cyanobacteria biodiversity increased, and the community shifted to co-dominance by multiple N-fixing species, including *Aphanizomenon flos-aquae*, *Cuspidothrix elenkinii*, *Dolichospermum crassum*, *Dolichospermum vigueri*, *Dolichospermum flos-aquae*, and *Dolichospermum sigmoidum*, with low concentrations of non-N-fixing taxa such as *Planktonlyngbya limnetica* and *Microcystis wesenbergii* (Figure 12b).

2020 had the greatest turnover in community composition relative to previous years, with decreased biodiversity and blooms dominated by *Aphanizomenon flos-aquae* from late June through late August, followed by late season growth of Woronichinia naegeliana, multiple *Dolichospermum* species, *Aphanocapsa* sp. and *Microcystis* spp. at non-bloom concentrations into the fall (Figure 12c). This compositional shift suggests that aeration has exacerbated N-limitation in Lake Carmi, favoring bloom-forming taxa that can access and fix N_2. In **2021**, early season blooms continued to be dominated by N-fixing taxa, including *Dolichospermum* spp. and *A. flos-aquae*, and Cuspidothrix sp. through late August. As in previous years, we saw a shift to coccoid non N-fixing taxa in the fall, with dominance by *Microcystis wesenbergii* (reported to be non-toxic) in early fall, and *Microcystis viridis* in late October (Figure 12d).

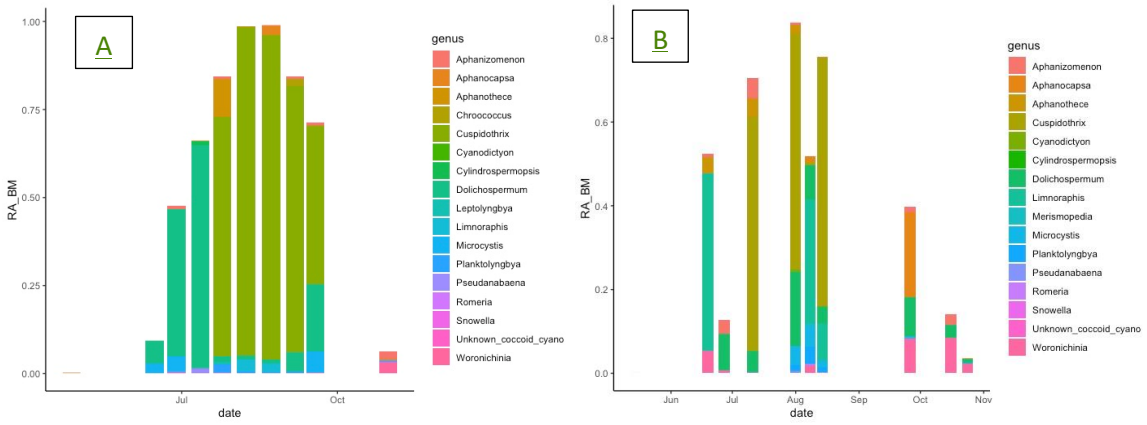

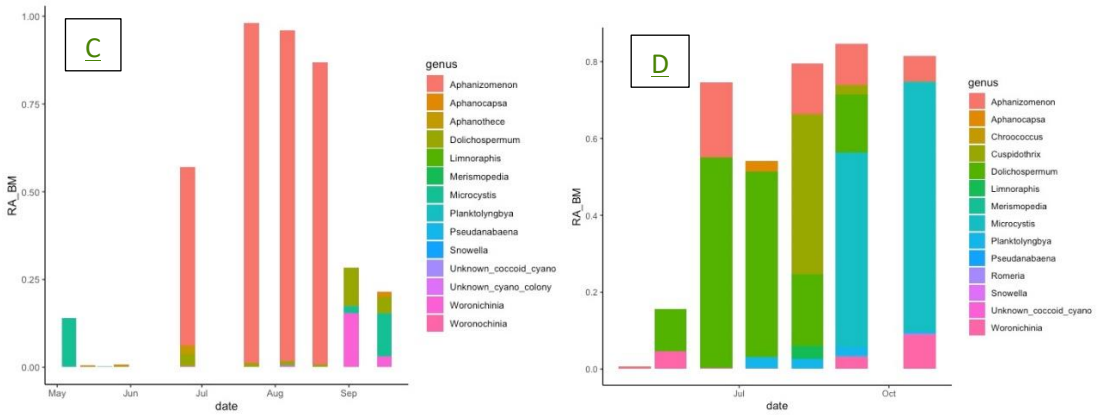

Figure 12 a - d. Cyanobacteria community composition and relative abundance at each sampling event in (a) 2018, (b) 2019, (c) 2020, and (d) 2021. Note that data are visualized as proportion of entire phytoplankton community, but only cyanobacteria are displayed here.

Because diatoms are excellent indicators of environmental change and saw significant biomass increase and community turnover post-aeration, we have included their community composition below as well. Pre-aeration in **2018**, the spring diatom bloom was dominated by the large centric taxa *Stephanodiscus niagare*, and chain-forming *Fragilaria crotenensis*, and *Asterionella formosa*, followed by increases in *Tabellaria flocculosa* in early summer and *Aulacoseira granulata* and *Acanthoceras* sp. in August. At late fall turnover, *S. niagare* returned (Figure 13a).

Like cyanobacteria assemblages, pre-aeration **2019** was similar to the spring diatom bloom of 2018, again dominated by *S. niagare* as well as *A. granulata*. This was followed by *Fragilaria crotenensis* (an indicator of nitrogen enrichment), then a small but diverse assemblage making up <10% of the overall phytoplankton biomass through summer and early fall. Late fall differed substantially from 2018. Here we saw a larger diatom bloom than in spring (generally we expect spring to be the larger bloom) dominated by *Aulacoseira granulata* and a smaller proportion of *S. niagare* (Figure 13b).

2020 differed in biomass and composition compared to previous years. The spring diatom bloom represented a greater proportion of overall biomass than in previous years, and was dominated by *Aualcoseira granulata* and *Asterionella formosa* through May. We saw a slight increase in diatom biomass in late June, then a second diatom bloom in September of *Aulacoseira granulata* and *Fragilaria crotenensis*, representing nearly 80% of total phytoplankton biomass (Figure 13c).

The diatom bloom in **2021** had similar biomass as 2020, but represented a smaller proportion of overall phytoplankton biomass due to increased cyanobacteria growth. Diatom composition differed from previous years, with the spring bloom composed of *Ulnaria* sp., *Stephanodiscus niagare*, *Asterionella formosa*, and *Aulacoseira granulata*. We saw an increase in *Ulnaria* sp. and *Aulacoseira granulata* through summer, suggesting frequent mixing events allowing them to

remain suspended in the water column. *Aulacoseira granulata* was the dominant species in the fall, though we did not observe a second diatom bloom as expected in the fall, instead this period was dominated by coccoid cyanobacteria (*Microcystis* spp., Figure 12d). This appears to correspond to an increase in sediment reactive phosphorus (Figure 8) and destabilization of the water column (Figure 4) following a period of hypolimnetic anoxia (Figure 5) starting in September (Figure 13d).

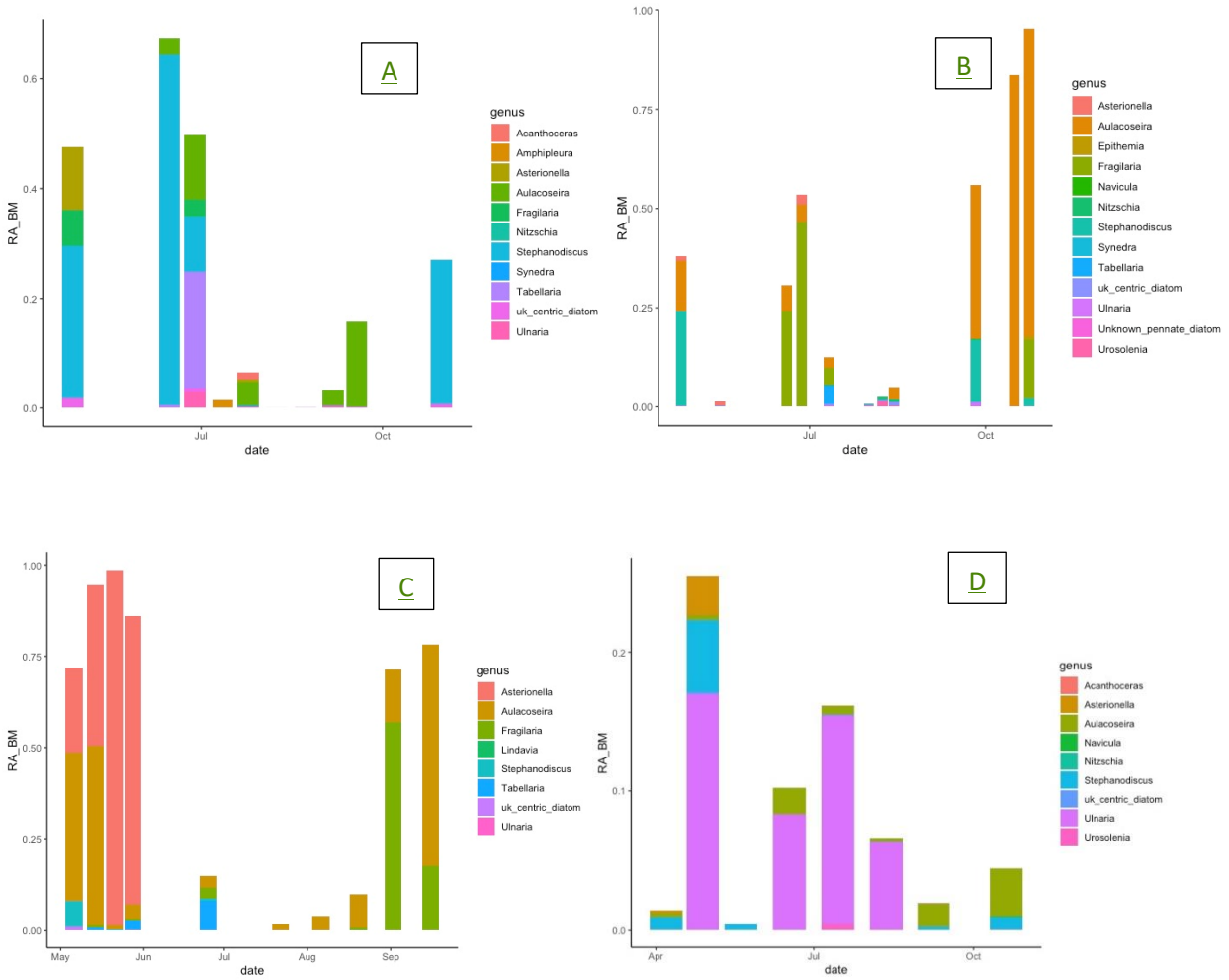

Figure 13 a - d. Diatom community composition and relative abundance at each sampling event in (a) 2018, (b) 2019, (c) 2020, and (d) 2021. Genera *Synedra* and *Ulnaria* are synonymous here due to a recent taxonomic reclassification. Note that data are visualized as proportion of entire phytoplankton community, but only diatoms (Bacillariophyceae) are displayed here.

In summary, cyanobacteria blooms have not been mitigated over 3 years of aeration, but instead have increased in 2020 and 2021. We saw significant inter-annual variability in phytoplankton assemblages between monitoring years, with increases in cyanobacteria and diatom biomass in 2020 and 2021, and further increases in cyanobacteria in 2021 that appear to have depressed the spring and fall diatom blooms. The spring diatom bloom represents an important early season event fueling zooplankton growth and upper trophic level productivity throughout the year. A trophic mismatch at this time could have cascading impacts on zooplankton and fish assemblages, as cyanobacteria are lower food quality and less palatable for consumers than diatoms. Lake Carmi cyanobacteria assemblages have been dominated throughout our monitoring period by nitrogen fixing taxa suggesting the lake is N- limited. Nitrogen limitation or N+P co-limitation is also supported by nutrient limitation bioassays conducted in Carmi in collaboration with GLEON in 2018 (Volopini et al. in review, Limnology and Oceanography). Aeration appears to have exacerbated N-limitation, shifting the lake from a relatively diverse algal community in 2018 and 2019 to dominance by fewer taxa and higher biomass blooms in 2020 and 2021 that displaced diatom blooms. Additionally, the significant increase in cyanobacteria biomass in 2021 may have shifted the community back towards late season P-limitation, evidenced by larger fall increases in coccoid, non N-fixing cyanobacteria taxa such as *Microcystis* spp. and *Woronichina* sp. Because of the high variability in algal community turnover between years, further seasonal microcosm or mesocosm bioassays are recommended to better understand algal response to nitrogen and phosphorus enrichment and altered lake mixing regimes.